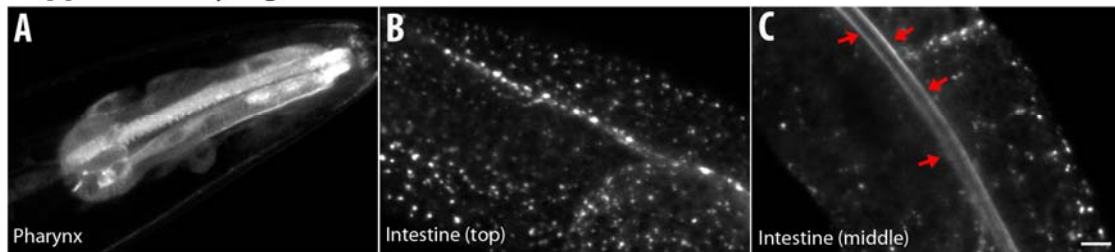


Supplemental Materials

Molecular Biology of the Cell

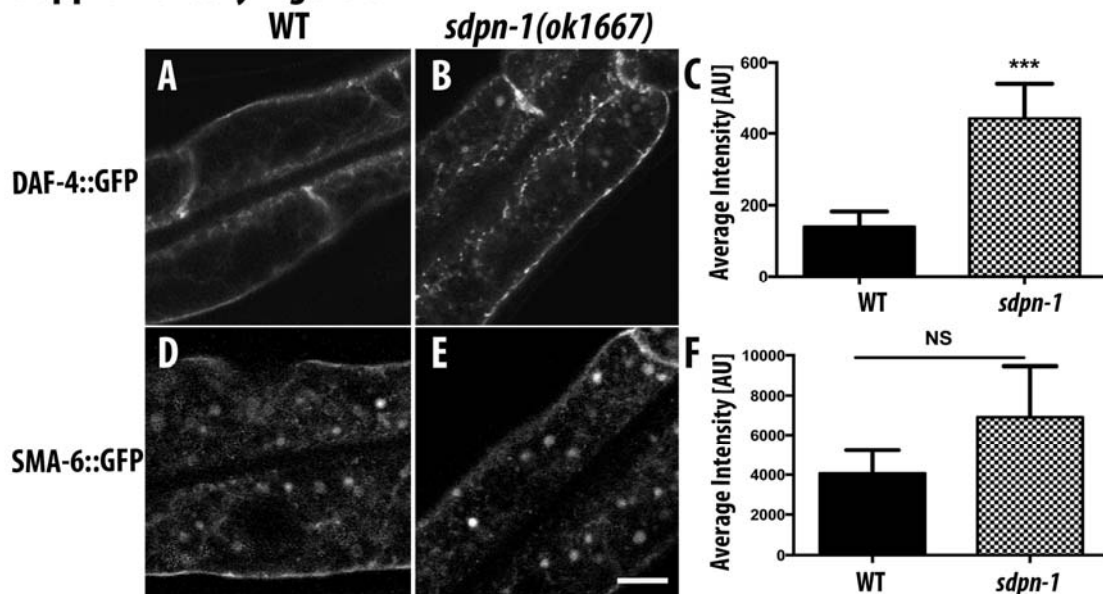
Gleason et al.

Supplementary Figure S1



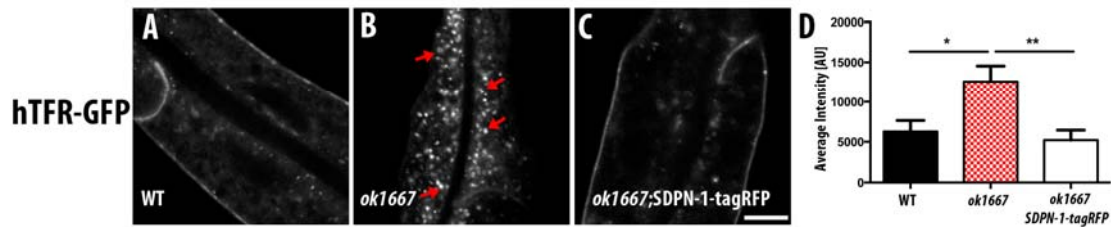
Supplemental Figure S1. Expression profile of SDPN-1 in *C. elegans*. Confocal images of the (A) pharynx, (B) intestine (top, *en face* basal view), and (C) intestine (middle, cross sectional view) arrows indicate the apical intestinal membrane. Scale bar 10 μ m.

Supplementary Figure S2



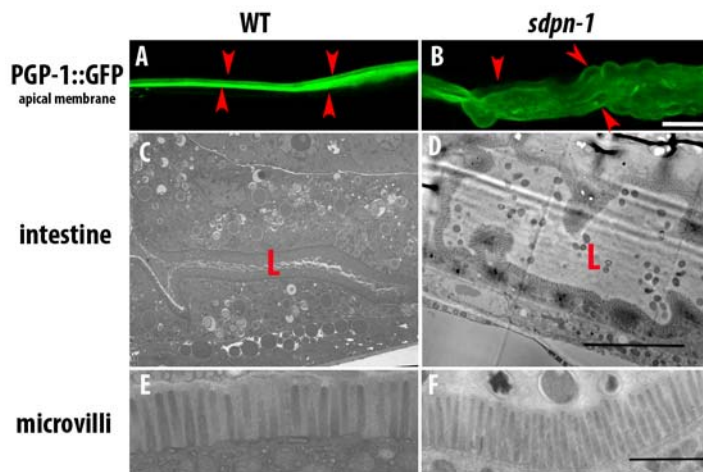
Supplemental Figure S2. *sdpn-1* mutants display differential trafficking effects on TGF-beta receptors DAF-4 (type I) and SMA-6 (type I). Loss of SPDN-1 function resulted in aberrant accumulations of (A-C) DAF-4::GFP (an ARF-6-dependent recycling cargo), but not (D-F) SMA-6::GFP (a retromer dependent cargo). n =6 animals. Error bars represent SEM:***P<0.001. Scale bar, 10 μ m.

Supplemental Figure S3



Supplemental Figure S3. Intestine-specific expression of SDPN-1::tagRFP rescues hTfR accumulation defects in *sdpn-1(ok1667)* null mutants. Confocal images of the intestine: (A) Control hTFR::GFP, (B) *ok1667*; hTFR::GFP, (C) and *ok1667*, hTFR::GFP, SDPN-1::tagRFP. Red Arrow indicate abnormal accumulations of hTFR::GFP. (D). Quantification of total intensity for micrographs. 6 animals for each genotype sampled in three different regions. of each intestine. Error bars represent SEM. * $P < 0.05$, ** $P < 0.01$ by analysis of variance (Beramendi *et al.*). Scale bar, 10 μm .

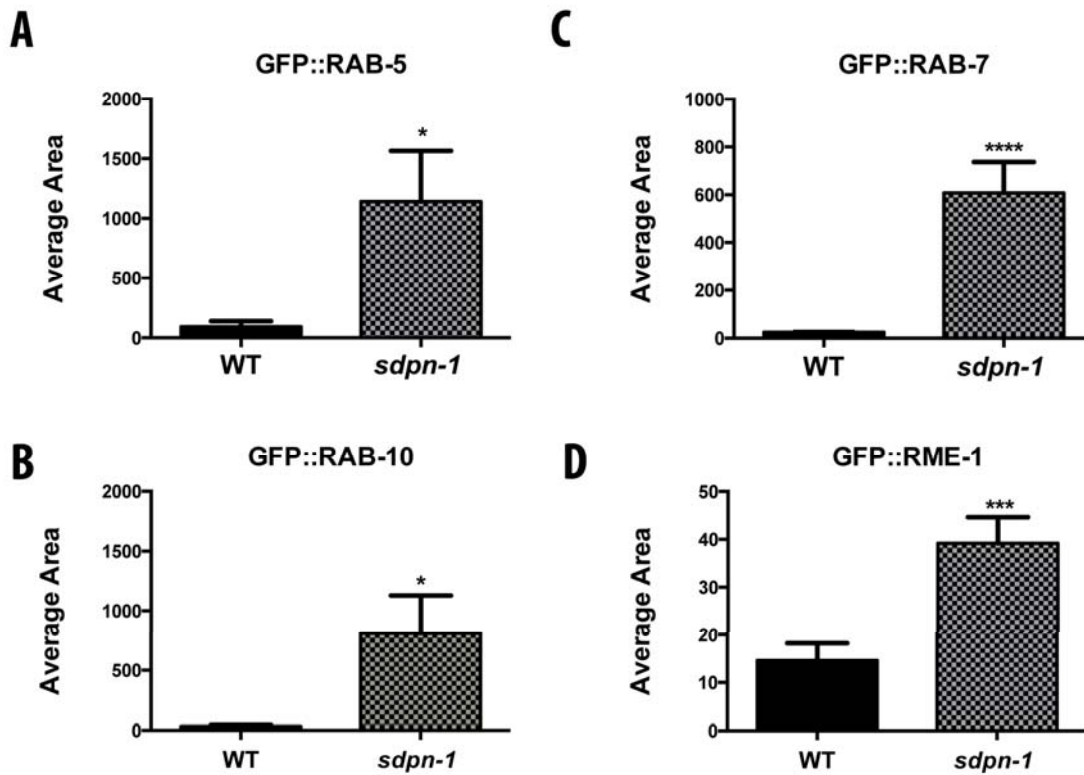
Supplemental Figure S4



Supplemental Figure S4. *sdpn-1* mutants display a convoluted intestinal lumen but normal microvilli. (A) 3D max projection of confocal micrographs representing the apical (luminal) membrane of about one cell length of intestine, marked with apical transmembrane protein PGP-1::GFP. The apical membranes are marked with red arrowheads in (A) wild-type, and (B) *sdpn-1* mutant. Note the abnormal shape of the apical membranes in *sdpn-1* mutant intestinal cells. (n=6)

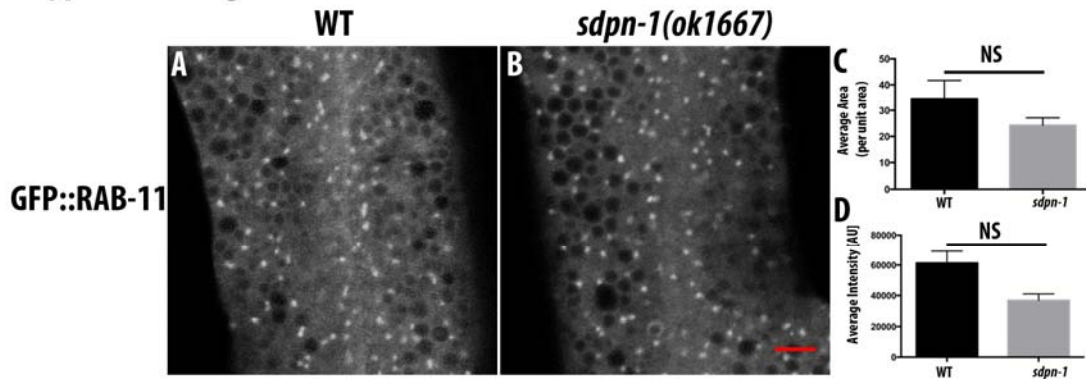
animals). Transmission electron micrographs showing longitudinal cross-sections through the intestine of young adult hermaphrodites in (C) wild-type, and (D) *sdpn-1* mutant. The lumen is marked with the letter L. Note the expanded lumen in the *sdpn-1* mutant. Panels E-F display higher magnification electron micrographs of a single apical intestinal membrane including microvilli. Microvilli of wild-type (E) and *sdpn-1* mutant (F) appear similar. Scale bar 10 μm (B), 5 μm (D), 1 μm (F).

Supplemental Figure S5



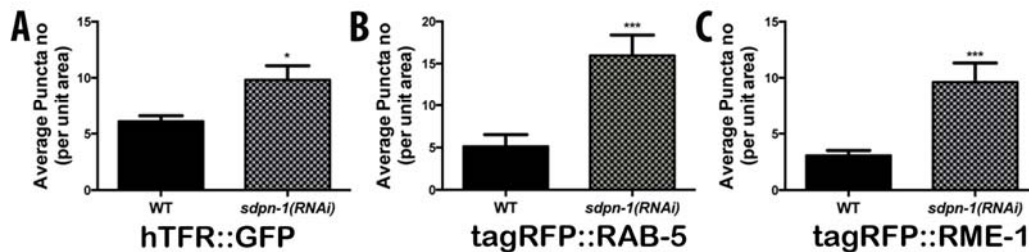
Supplemental Figure S5. Average area covered for GFP-labeled endosomal compartment markers. Quantification of the average area (per unit region) positive for GFP-labeled endosomal compartments depicted in main Figure 3. (A) GFP::RAB-5, (B) GFP::RAB-7, (C) GFP::RAB-10, (D) GFP::RME-1. Error bars represent SEM. * $P < 0.05$, *** $P < 0.001$, **** $P < 0.0001$ (student's t-test). 6 animals of each genotype sampled in three different regions of each intestine positioned at random.

Supplemental Figure S6



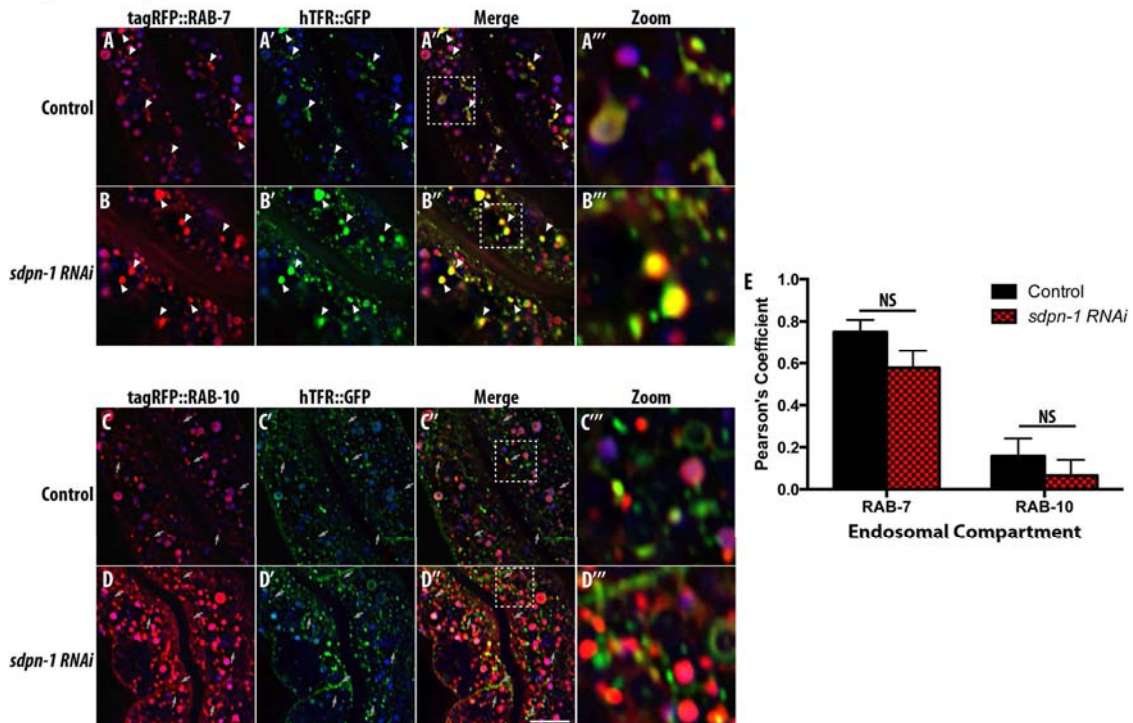
Supplemental Figure S6. *sdpn-1* mutants did not disrupt GFP::RAB-11 apical recycling endosomes. Apical recycling endosomes remained normal in *sdpn-1* (*RNAi*) mutants. All images are laser scanning confocal micrographs of the worm intestine expressing GFP::RAB-11. (A&B) Expression and morphology of GFP::RAB-11 labeled structures in *sdpn-1*(*RNAi*) remained comparable to wild-type. Statistical analysis: (D) Average puncta size (per unit area) and (E) Average Intensity (per unit area). Error bars are SEM. 6 animals of each genotype sampled in three different regions of each intestine positioned at random. Scale bar, 10 μ m.

Supplemental Figure S7



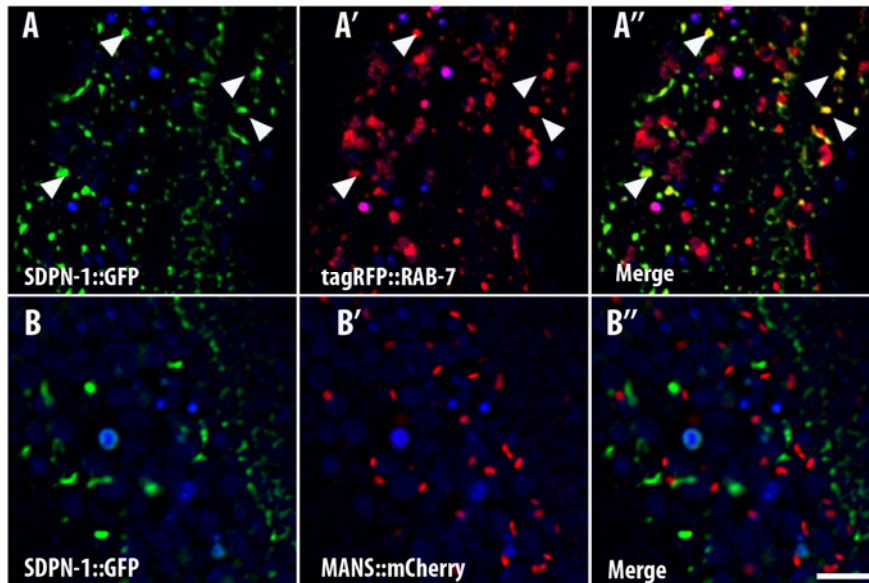
Supplemental Figure S7. Average puncta number increases for recycling cargo hTFR and early and basolateral recycling endosomal compartments after *sdpn-1*(*RNAi*). (A) hTFR::GFP, (B) tagRFP::RAB-5, (C) tagRFP::RME-1. Error bars represent SEM. * $P < 0.05$ and *** $P < 0.001$ (student's t-test). 6 animals of each genotype sampled in three different regions of each intestine positioned at random.

Supplemental Figure S8



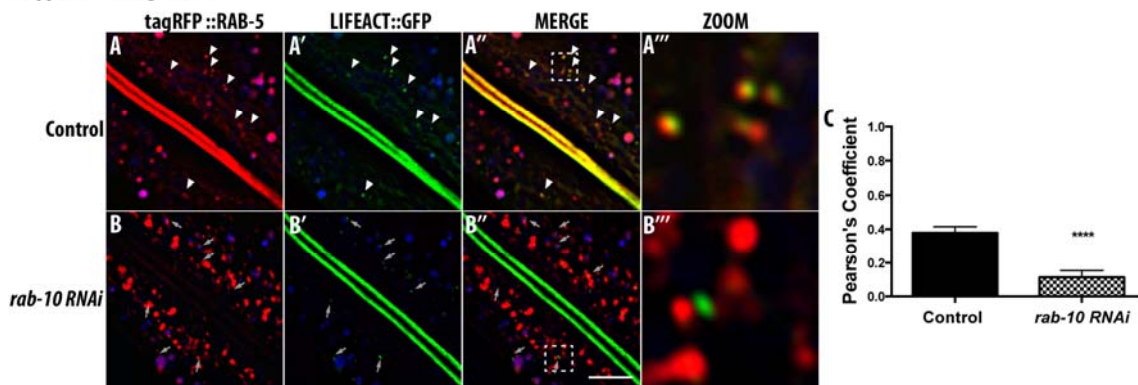
Supplemental Figure S8. Lack of change of hTFR::GFP colocalization with tagRFP::RAB-7 or tagRFP::RAB-10 after *sdpn-1* RNAi. Representative images of (A-A'') control animals (B-B'') *sdpn-1(RNAi)* animals expressing recycling cargo hTFR::GFP and tagRFP::RAB-7. White arrow heads depict positive overlap. Representative images of (C-C'') control animals (D-D'') *sdpn-1(RNAi)* animals expressing recycling cargo hTFR::GFP and tagRFP::RAB-10. Grey arrows indicate recycling cargo hTFR devoid of RAB-10. In each image autofluorescent lysosome-like organelles appear in in all three channels (including blue), whereas GFP appears only in the green channel and RFP appears only in the red channel. Green and red signal that does not overlap with the blue channel represent pure GFP and RFP signals respectively. (E) Pearson's correlation coefficient for each endosomal compartment. n =6 animals. Error bars represent SEM. Scale bar, 10 μ m.

Supplemental Figure S9



Supplemental Figure S9. SDPN-1 is occasionally overlaps with RAB-7 and is not enriched on Golgi. (A-A'') SDPN-1::GFP partially colocalizes with RAB-7-labeled puncta but not RAB-7-labeled rings. (B-B'') SDPN-1::GFP is not found on Golgi structures (n =6 animals). All micrographs are from deconvolved 3D confocal image stacks acquired in intact living animals expressing intestinal specific GFP and RFP-tagged proteins. Scale bar, 10 μ m.

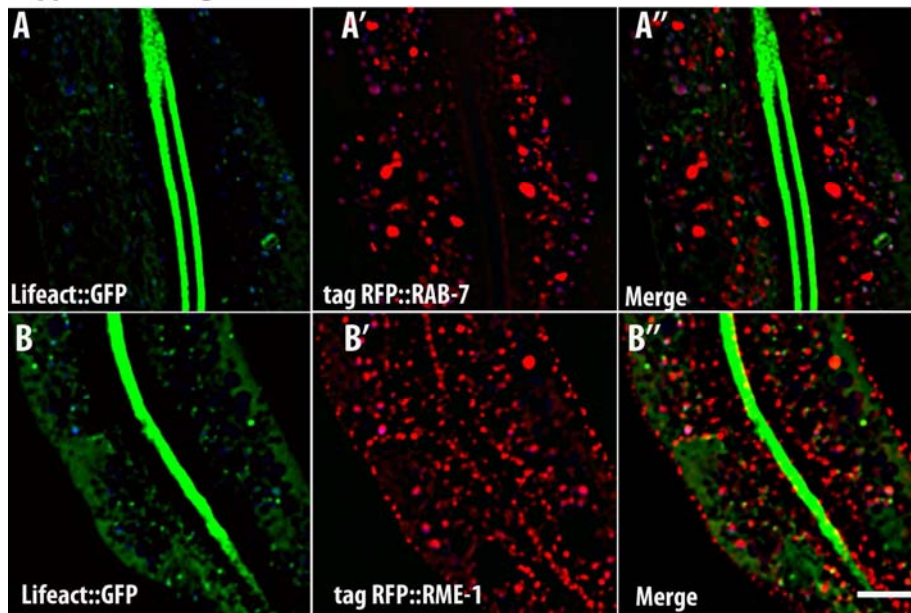
Supplemental Figure S10



Supplemental Figure S10. RAB-10 function is important for recruitment of filamentous actin to early endosomes. All micrographs are from deconvolved 3D confocal image stacks acquired in intact living animals expressing intestinal specific GFP-tagged recycling cargo LifeAct-GFP and

tagRFP-RAB-5. (A-A'') In control animals, LifeAct::GFP positive puncta often colocalize with tagRFP::RAB-5 labeled early endosomes. White arrowheads indicate positive colocalization. (B-B'') A striking decrease in localization of LifeAct::GFP and tagRFP::RAB-5 was seen in *rab-10(RNAi)* animals. Grey arrows indicate early endosomes depleted of filamentous actin. In each image autofluorescent lysosome-like organelles appear in in all three channels (including blue), whereas GFP appears only in the green channel and RFP appears only in the red channel. Green and red signal that does not overlap with the blue channel represent pure GFP and RFP signals respectively. (C) Pearson's correlation coefficient for colocalization of LifeAct::GFP with tagRFP::RAB-5. n=6 animals. Error bars represent SEM. ****P<0.001 (student's t-test) Scale bar, 10 μ m.

Supplemental Figure S11



Supplemental Figure S11. LifeAct-positive puncta do not colocalize well with RAB-7 or RME-1. All micrographs are from deconvolved 3D confocal image stacks acquired in intact living animals expressing intestinal specific GFP and RFP-tagged proteins. (A-A'') LifeAct::GFP is not found on tagRFP::RAB-7-labeled late endosomes nor (B-B'') tagRFP::RME-1 labeled basolateral recycling endosomes. (n =6 animals). Scale bar, 10 μ m.

Table S1. Transgenic and mutant strains used in this study

pwIs72[Pvha-6::GFP::RAB-5](Chen et al., 2006)
pwIs87[Pvha-6::GFP::RME-1] (Chen et al., 2006)
pwIs170[Pvha-6::GFP::RAB-7] (Chen et al., 2006)
pwIs206[Pvha-6::GFP::RAB-10] (Chen et al., 2006)
pwIs722[Pvha-6::SDPN-1::GFP] (Pant et al., 2009)
pwIs1257[Pvha-6::LifeactGFP] this work
pwIs1258[Pvha-6::Lifeact-tagRFP] this work
pwIs911 [Pvha-6::MIG-14::GFP](Shi et al., 2009)
pwIs112[Pvha-6::hTAC::GFP] (Chen et al., 2006)
pwIs717[Pvha-6::hTfR::GFP] (Sun et al., 2012)
pwIs921[Phva-6::SMA-6::GFP] (Gleason et al., 2014)
pwIs922[Pvha-6::DAF-4::GFP] (Gleason et al., 2014)
pwIs1196[Pvha-6::SS::GFP::CD4-dileucine] this work
pwIs846[Pvha-6::RFP::RAB-5] (Shi et al., 2007)
pwIs849[Pvha-6::RFP::RAB-7] (Gleason et al., 2014)
pwIs957[Pvha-6::RFP::RAB-10] (Sun et al., 2012)
pwIs852Pvha-6::RFP::RME-1] (Shi et al., 2007)

sdpn-1(ok1667) From C. elegans Knockout consortium